

Probing Macrophage Activity with Carbon-Nanotube Sensors**

Iddo Heller, Wiljan. T. T. Smaal, Serge G. Lemay, and Cees Dekker*

Electronic sensors based on individual single-walled carbon nanotubes (SWNTs) provide an excellent opportunity to expand the existing set of electrical probes available for single-cell studies with a versatile high-sensitivity probe of nanometer dimension. SWNTs have been shown to function both as nanoscale electrochemical sensors and as electrostatic field-effect-transistor (FET) sensors.^[1–3] The biological processes occurring in and around living cells are commonly of electrostatic and/or electrochemical nature, and can thus potentially be probed with SWNT sensors. Importantly, SWNTs have a quasi-one-dimensional cylindrical geometry.^[4] With a length of several micrometers, a SWNT can span a single cell, while its diameter is of the order of one nanometer, directly comparable to the size of single proteins. In comparison with current electrical probes that have lateral dimensions comparable to single cells,^[5] SWNT probes can have a higher spatial resolution and impose a largely reduced physical perturbation when in contact with or puncturing through the membrane of a single cell.

Here we present our first studies of SWNT sensors as electrical probes to interrogate single macrophage cells and probe cellular activity. As part of the immune system, macrophages can ingest and digest pathogens in a process known as phagocytosis.^[5] We coat SWNT sensors with antibodies to stimulate macrophages to attach to, ingest, and attempt to digest the sensors. During phagocytosis a multitude of processes occur, including binding of antibodies to membrane-bound receptors, changes in cell morphology, pH changes, and the production of cytotoxic molecules. By employing antibody-coated SWNTs in an electrolyte-gated transistor configuration,^[6] we aim to follow the process of phagocytosis in real-time by simultaneously monitoring both changes in transistor conductance (FET signal) and changes in

the electrochemical current (EC signal). The SWNTs are suspended above the substrate to allow close contact between the cell and the SWNT.^[7] We present experiments that display FET and EC responses after cell adhesion, which suggests successful detection of cellular activity. The performance of the SWNT sensors in an as-fabricated layout is, however, not optimal: we find that the FET signal of suspended, contact-passivated SWNT transistors is often unstable and that electrochemical reactions at the SWNT electrodes are suppressed. We show that the detection of electrochemical signals from single cells can be enhanced when the SWNT is coated with catalytic platinum nanoparticles. Finally, we discuss the prospects of SWNTs as electrical probes to study single cells.

Figure 1a shows the experimental device layout used to study the detection of macrophage activity. We use a SWNT in a contact-passivated, suspended layout.^[8,9] SWNT transistors are fabricated on oxidized silicon wafers by lithographically defining Cr/Au electrodes that electrically contact chemical-vapor-deposition (CVD)-grown SWNTs. Windows in a poly (methyl methacrylate) (PMMA) passivation layer are opened up to partially expose the SWNTs,^[9] after which a buffered HF etch is used to suspend the SWNT above the SiO₂ substrate.^[7] The suspended segment of the SWNT allows the macrophage cell to engulf the SWNT. Although the exact geometry of the cell engulfing the SWNT is not known, phagocytosis of the SWNT sensor entails an incomplete swallowing of the SWNT due to the device layout. Variations to this layout are discussed later. The substrate with SWNT devices is placed in a home-built flow-cell on top of a Peltier element to maintain the temperature at about 37 °C. The flow cell allows access for an Ag/AgCl (3M NaCl) reference electrode^[10] and contains a poly(dimethylsiloxane) PDMS microchannel that confines the solutions and cells to the active sensor area. Figure 1b shows a section of the PDMS channel centered on multiple, individually addressable SWNT transistors of which the Au source (vertical) and drain (horizontal) electrodes are visible. The positions of six SWNT sensors are indicated by the dashed circles. To introduce macrophage cells, cell suspensions are injected into the PDMS channel. In Figure 1b, multiple macrophage cells can be seen adhering to the device surfaces. By controlling the flow direction in the channel, individual macrophage cells that are in suspension can be accurately positioned over the SWNT sensor, after which the flow is stopped to allow cells to precipitate and adhere to the sensor surface. Figure 1c shows a macrophage cell that was positioned on top of a SWNT transistor. The

[*] Prof. Dr. C. Dekker, Dr. I. Heller, W. T. T. Smaal, Prof. Dr. S. G. Lemay Section Molecular Biophysics, Kavli Institute of NanoScience, Delft University of Technology
Lorentzweg 1, 2628 CJ Delft (The Netherlands)
E-mail: c.dekker@tudelft.nl

[**] This work was supported by the Nederlandse Organisatie voor Wetenschappelijk Onderzoek (NWO), and NanoNed. The authors would like to thank Herman P. Spaik for useful discussions and Diederik van de Wetering for assistance with the THP-1 cell cultures.

Supporting Information is available on the WWW under <http://www.small-journal.com> or from the authors.

DOI: 10.1002/sml.200900823

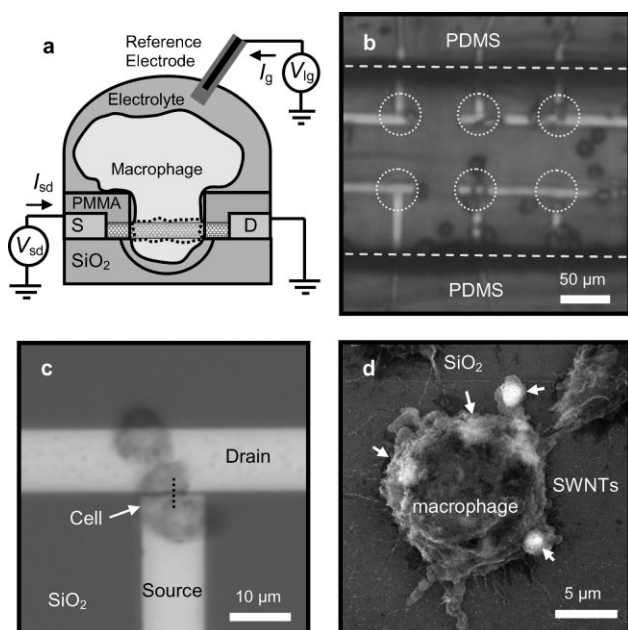


Figure 1. Experimental layout of the SWNT sensors and their interface with macrophage cells. a) Schematic side view of a SWNT sensor in contact with a macrophage cell. A SWNT is electrically contacted by source and drain electrodes that are insulated from the electrolyte by a layer of PMMA. The SWNT is suspended 100–150 nm above the SiO₂ substrate. $V_{sd} = 10$ mV is applied while I_{sd} is monitored. V_{lg} is applied to the electrolyte through an Ag/AgCl reference electrode inserted in solution, and I_{lg} is recorded to monitor electrochemical reactions. b) Microscopy top view image of a section of the PDMS-channel located in a home-built flow-cell centered on the chip that contains multiple SWNT transistors. The dashed lines indicate the boundaries of the PDMS channel. The dashed circles show the location of six SWNT transistors. On average there is roughly one SWNT per transistor. The dark spherical objects in the channel are THP-1 macrophage cells that adhere to the substrate. c) Higher magnification microscopy image of THP-1 cells on a SWNT transistor. The dotted line depicts the location of a SWNT transistor. This picture was taken after the cells were fixed using isopropanol and the device was dried on a hotplate. d) SEM image of a THP-1 cell on top of CVD-grown SWNTs that were coated with IgG antibodies. Polystyrene beads were added to test phagocytic activity. The arrows indicate locations of beads that were ingested by the cell. The cell was fixed and dried as in (c).

approximate location of a SWNT is indicated by the black dotted line that bridges the micrometer-sized gap between source and drain electrodes.

In our study, murine RAW 264.7 cells and human THP-1 cells were used as model systems for macrophage cells, as described further in the experimental section. We first tested the compatibility of macrophages with SWNT sensors. We found that THP-1 cells were viable and still capable of phagocytosis 96 h after phorbol-12-myristate-13-acetate (PMA)-stimulated differentiation on SiO₂, Au, and SWNT substrates. Highest densities of cells were found on sections of these substrates that were coated with IgG antibodies (Sigma-Aldrich, I4506). Figure 1d shows a scanning electron microscopy (SEM) image of a differentiated THP-1 cell on CVD-grown SWNTs coated with IgG. The arrows point to the locations of ingested polystyrene beads that confirm phagocytic activity. From these experiments we conclude that macro-

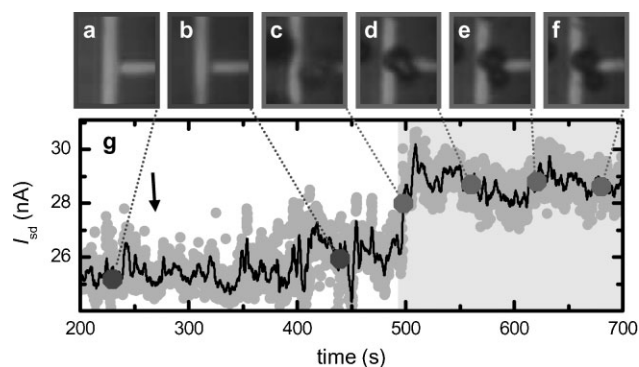


Figure 2. Attachment of a RAW macrophage on a suspended, contact-passivated SWNT transistor coated with IgG. a–f) Microscopy images of a SWNT device taken during the attachment of a RAW macrophage cell. g) The FET signal, I_{sd} , as a function of time recorded during the adsorption of RAW macrophage on top of the device. The grey dots represent I_{sd} sampled and averaged over 40 ms time intervals while the black line is the 20-point running average of the grey data points. The black arrow indicates the moment in time at which the cell suspension is injected into the PDMS channel. The shaded background of the graph represents the time course over which a cell was confirmed to be present over the device by microscopy. Large dots indicate the times at which the corresponding images of (a–f) were taken.

phages maintain viability and are capable of phagocytosis in the presence of the materials used to construct the SWNT sensors.

We now turn to the electrostatic detection of macrophage activity using SWNT sensors. Figure 2 shows an experiment where a RAW cell adheres to a sensor that consists of a single suspended semiconducting SWNT with PMMA-passivated contacts. Prior to the experiment, RAW cells were mechanically harvested from a cell-culture flask after thorough washing with phosphate buffer saline (PBS) and subsequently concentrated in PBS by centrifugation. The SWNT sensor was incubated with 1 μ M murine IgG (Sigma-Aldrich, I5381) before introducing the RAW cells. Images of the device in the PDMS channel that were acquired during the measurement are displayed in Figure 2a–f. The FET signal plotted in Figure 2g shows the source–drain current, I_{sd} , that passes through the SWNT at constant source–drain voltage $V_{sd} = 10$ mV and a liquid-gate voltage $V_{lg} = -350$ mV versus Ag/AgCl. The blue and red dots in Figure 2g indicate the time at which each image is taken. In Figure 2a and b no cell is present near the SWNT sensor. The black arrow in Figure 2g indicates the time when the cell suspension was injected into the PDMS channel, showing no immediate FET response. The background of the plot in Figure 2g is highlighted in yellow during the time course that the cell resided over the SWNT device, as visible in Figure 2c–f. As is obvious from the FET signal in Figure 2g, an increase of device conductance is correlated with the presence of a cell on top of the SWNT device. In the Supporting Information (Figure S1) we show a second device that reveals FET changes over longer timescales after adhesion of THP-1 macrophages. Caution is warranted in directly attributing changes in FET signal to cellular activity: we found that the conductance of suspended and contact-passivated SWNT transistors in electrolyte solution is more unstable than that of non-suspended and/or non-passivated transistors. In the Supporting Information

(Figure S2) we show that sizeable fluctuations of the FET signal can occur for the device of Figure 2 before and after cell adhesion. The cause of this instability is unknown. Despite these difficulties, the experiment of Figure 2 is highly suggestive that the presence of a macrophage cell can be detected by the FET sensor.

Next we discuss electrochemical detection of macrophage activity. In the process of phagocytosis, macrophages generate reactive oxygen species (ROS) and reactive nitrogen species (RNS). Amatore et al.^[5,11] previously demonstrated that ROS and RNS excreted by cells can be detected by amperometry using platinized carbon-fiber electrodes. The different ROS and RNS species (H_2O_2 , ONOO^- , NO , and NO_2^-) exhibit well-separated oxidation waves at potentials ranging between -300 mV and -900 mV versus Ag/AgCl (here we use the convention that potentials are applied to the Ag/AgCl reference electrode with respect to the working electrode).^[11] H_2O_2 can be oxidized at potentials more negative than -300 mV versus Ag/AgCl.^[11] In control experiments we find, however, that significant electrochemical oxidation of H_2O_2 cannot be reproducibly detected on contact-passivated SWNT sensors at small overpotentials ($V_{\text{lg}} \geq -600$ mV versus Ag/AgCl). Supporting Information Figure S3 shows an example where a contact-passivated, suspended SWNT sensor displays no EC signal change in response to flushing a solution of 1 mM H_2O_2 . Measuring at more negative oxidative potentials than -600 mV versus Ag/AgCl is not desirable since this significantly decreases the signal-to-noise ratio of the FET signal.^[12]

Since Amatore et al. have previously found that effective electrochemical detection of ROS and RNS species using carbon electrodes requires the electrodes to be platinized,^[11] we tested the electrochemical performance of platinum as electrode material. Figure 3 shows an experiment where a differentiated THP-1 cell is located on an unsuspended SWNT transistor with exposed Pt contact electrodes (see inset Figure 3a). Figure 3a and b show the simultaneously recorded FET signal (I_{sd}) and EC signal (gate current, I_{g}), respectively, at constant $V_{\text{lg}} = -600$ mV versus Ag/AgCl. The blue background in Figure 3 highlights two distinct events in the EC signal. The events consist of a rapid increase in oxidative current of ≈ 30 pA, followed by a slow decrease with a half-life time of ≈ 20 s. Although the observed changes in FET signal roughly correlate to the events in the EC signal, at present these cannot be exclusively related to cellular activity. The events in I_{g} represent a detected charge of ≈ 1 nC. The corresponding number of electronic charges per event is ≈ 10 femtomole. Similar events measured by Amatore^[5,11,13] and Yoshimura^[14] were attributed to excretion of ROS and RNS, where the relatively long time scales and magnitude of the events led them to conclude that the events are not related to individual vesicular release events, but rather to the active production of membrane-permeable ROS/RNS like H_2O_2 . The increase in oxidative current after adhesion of a THP-1 macrophage to the SWNT sensor with exposed contacts as displayed in Figure 3 is suggestive of the excretion of ROS and RNS. Most of the oxidative current likely arises, however, from electrochemical conversion at the Pt contact electrodes. The data obtained in this experiment are consistent with extracellular detection of ROS/RNS from macrophages with micrometer-sized electrodes.

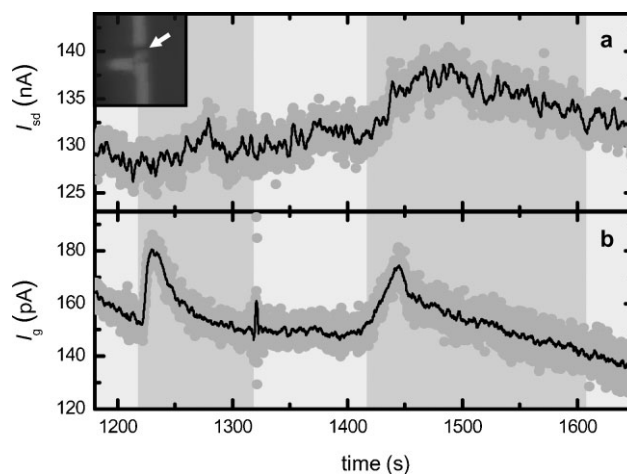


Figure 3. FET and EC signal recorded while a PMA-differentiated THP-1 macrophage, harvested through trypsinization, was present on a non-suspended SWNT transistor with exposed Pt contacts. a) I_{sd} as function of time. b) I_{g} as a function of time. The cell was found to adhere to the device at $t = 0$ s. In (a) and (b), the grey dots represent the current sampled and averaged over 40 ms and the black solid line is the 20-point running average of the grey data points. The white background in (a) and (b) indicates that a cell is present on the device over the entire plotted time range, where the grey bands highlight the time course over which two events were observed in I_{g} . The transiently decreasing I_{g} observed before $t = 1220$ s is caused by a flush of PBS at $t = 1100$ s. The spike near $t = 1320$ s is caused by opening and closing of the Faraday cage in which the setup is contained. The inset in (a) shows the SWNT transistor device, where the white arrow points to a (poorly visible) THP-1 cell.

To enhance the electrochemical detection of ROS and RNS with SWNTs while maintaining the nanometer size of the electrode, we have deposited electrically contacted platinum nanoparticles on the SWNTs.^[15–17] In Figure 4a and b, we show a SWNT transistor before and after platinization, respectively. Here, Pt was deposited on the SWNTs by applying a liquid-gate potential of 1 V during 10 s in a PBS solution with 1 mM K_2PtCl_4 . As visible in Figure 4b, Pt was deposited on the SWNTs in the form of electrically contacted nanoparticles approximately 25 nm in diameter. SWNT devices coated with Pt nanoparticles can still function as FET sensors since their conductance is affected by the electrolyte-gate potential.

Figure 4c shows a measurement of the EC signal measured with a suspended, contact-passivated SWNT transistor at constant $V_{\text{lg}} = -700$ mV versus Ag/AgCl in the presence of a THP-1 macrophage. As demonstrated in Reference [11] this potential allows for the electrochemical detection of H_2O_2 , ONOO^- , and NO . The SWNT sensor was first coated with Pt identical to the SWNT device in Figure 4b and subsequently coated with murine IgG as previously described. Prior to this experiment, we amperometrically confirmed that the sensor is sensitive to the presence of H_2O_2 , yielding an oxidative current of ≈ 10 pA for the electrochemical oxidation of 1 mM H_2O_2 in RPMI medium (see Supporting Information Figure S4). At $t = 850$ s, RPMI was flushed through the PDMS channel. Subsequently, from $t = 2000$ s to $t = 2500$ s, THP-1 cells suspended in RPMI were injected into the channel. From approximately $t = 2400$ s a macrophage cell was present over the SWNT sensor. After approximately 400 s, a series of spikes

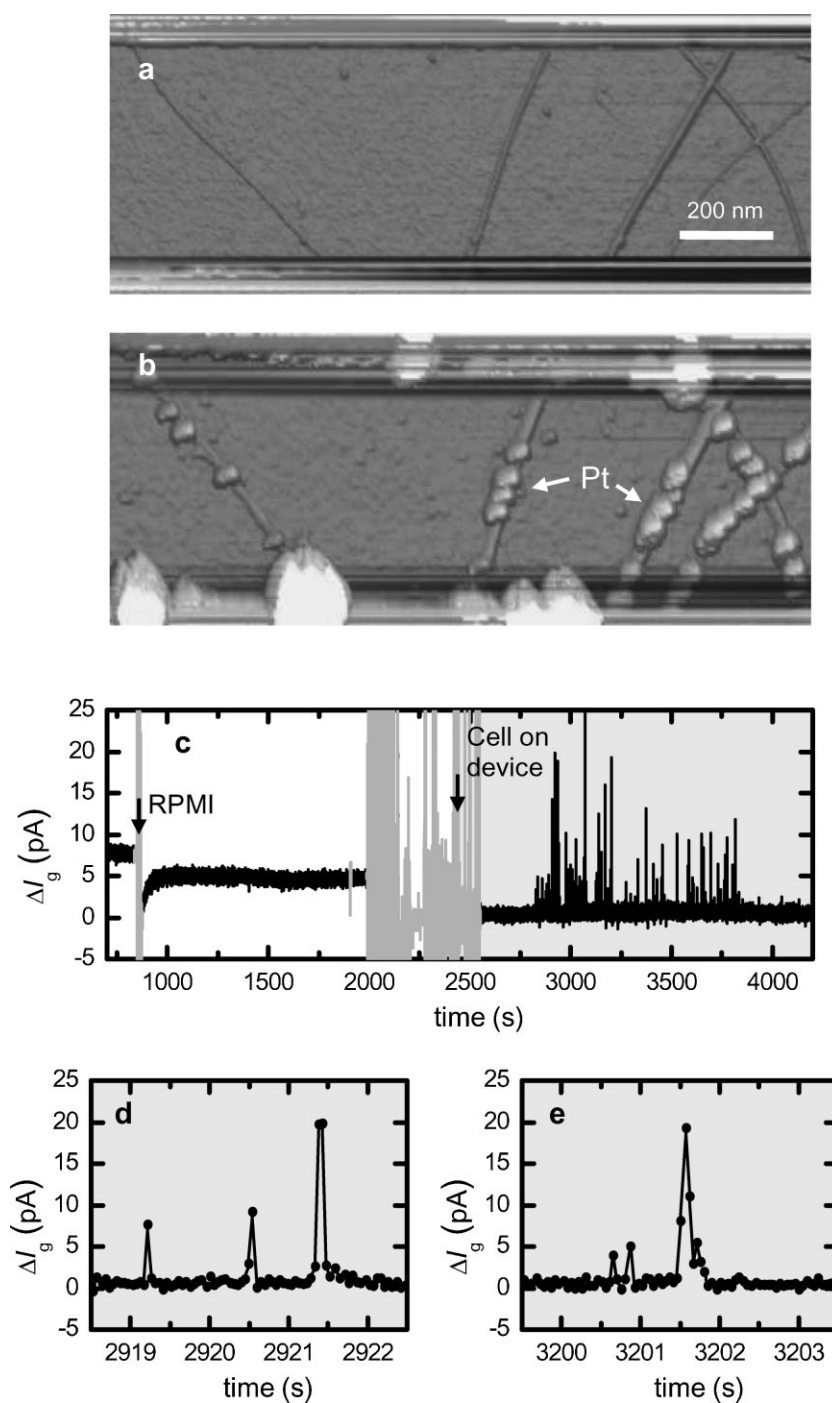


Figure 4. Platinization of SWNTs and detected EC signal in the presence of THP-1 macrophages. a) Atomic force microscopy (AFM) image of a pristine SWNT transistor with exposed contacts. b) AFM image of the same SWNT device after deposition of Pt. The white arrows point to some of the deposited Pt nanoparticles. c) ΔI_g as a function of time measured at $V_{lg} = -700$ mV versus Ag/AgCl with a suspended, contact-passivated device after Pt coating similar to (b) and subsequent IgG coating. Note that for this device, which consists of two SWNTs, the Au electrodes might have been partially exposed during fabrication. Grey and black data indicate I_g sampled and averaged over 40 ms time intervals, where the data depicted in grey show increased noise related to manipulation of the fluid flow. The black arrows near $t = 850$ s indicates flushing of RPMI solution, while the black arrow near $t = 2400$ s indicates the moment a THP-1 cell covers the SWNT device. The graph background is shaded over the time course where the cell is present over the device. d, e) Zoomed-in plot of 4 s time intervals of the data in (c). Here the black dots indicate the ΔI_g data points as sampled and averaged over 40 ms time-intervals while the solid line interconnects the points. In (c–e) a baseline current was subtracted.

was detected in the electrochemical current. Figure 4d and e shows two zoomed-in plots of the observed spikes. The events occur on much shorter time scales than the events observed in Figure 3: here, the observed peak height varies between ≈ 5 pA and ≈ 20 pA and the peak duration varies from below the time resolution of 40 ms to up to ≈ 1 s. The individual peaks thus represent ≈ 1 pC, or ≈ 10 attomole of electronic charges, which is comparable to the amount of charge previously reported for individual vesicular release events.^[18,19] Further studies are required to warrant unequivocal biological interpretation of the observed spikes. We currently presume, however, that these sharp bursts are representative for the vesicular release of ROS/RNS.^[19] From this experiment, we conclude that SWNT devices can be coated with Pt nanoparticles and function as sensitive electrochemical sensors that can enhance the detection of ROS/RNS excreted by macrophages.

In summary, we have studied the feasibility of detecting macrophage activity with SWNT sensors. We found that in a suspended, contact-passivated layout, the FET signal is unstable. In addition, the sensitivity of the SWNT sensor for electrochemical oxidation of ROS/RNS is not optimal. Nevertheless, using unmodified devices we have observed signals in the presence of single macrophage cells, both in FET response and EC response, that are highly suggestive of cellular activity. We have shown that SWNTs can be coated with Pt nanoparticles to significantly enhance the sensitivity for electrochemical oxidation of ROS/RNS. Events observed with Pt-coated SWNTs are suggestive of vesicular release of ROS/RNS. Because in this layout Pt nanoparticles are electrically contacted on a suspended SWNT, the macrophage can engulf and ingest the electroactive sensor, which offers the opportunity to electrically monitor the processes that occur during phagocytosis of pathogens from within the cell.

In general, SWNT sensors have potential as powerful tools for studying single cells, primarily because of their dimensions. The combination of a micrometer-scale length and a nanometer-scale diameter allow them to function as nanoscale wires that electrically contact the interior of living cells with minimal perturbation and maximal spatial resolution. In addition, SWNTs can simultaneously function as electrostatic and electrochemical sensors, allowing

simultaneous gathering of multiple types of information with one sensor. It is, however, important to realize that electrochemical gating of SWNTs and electrochemistry are inevitably coupled.^[20] Consequently, the optimal V_{lg} for EC detection might not coincide with the optimal V_{lg} for FET measurements. In the specific case of the experiments with macrophages presented here, electrochemical oxidation of ROS/RNS requires $V_{lg} < -300$ mV versus Ag/AgCl, while maximal FET sensitivity is in the sub-threshold regime of conductance (typically around 0 V versus Ag/AgCl).^[12]

Several important points need to be further studied and improved before we can use SWNT sensors as practical tools to study cells. First, the stability issues reported here need to be resolved. Furthermore, the sensitivity and specificity of sensing need to be considered. Bare SWNTs are not necessarily very sensitive to the processes of interest, as was the case here for the oxidation of ROS and RNS. Also, bare SWNTs are not expected to be very specific for detection of only one process inside cells. Coating of SWNTs can help resolve the issues related to specificity and sensitivity. As we show here, a catalytic Pt nanoparticle coating can enhance the sensitivity for certain electrochemical processes. Alternatively, SWNTs can be interfaced with antibodies and other receptors to enhance both specificity and sensitivity for certain processes.^[21–24] SWNT sensors thus can be versatile nanoscale tools to study the interaction of immobilized biomolecules with their natural environment, the living cell. As demonstrated here, however, further work is required before SWNTs can live up to this exciting prospect.

Experimental Section

Cell cultures: The monocytic suspension cell-line THP-1 (ECACC, 88081201) was cultured in RPMI 1640 medium (Gibco, 22409-015), supplemented with 10% fetal bovine serum (FBS, Greiner, 758093), L-glutamine (Invitrogen, 25030-024), and penicillin/streptomycin (Invitrogen, 15070-063), and incubated at 37 °C in 5% CO₂ atmosphere. Incubation of THP-1 monocytes with PMA (Sigma–Aldrich P1585) for 1 to 2 days stimulates the cells to differentiate into adherent macrophage-like cells capable of phagocytosis.^[25] The adherent murine macrophage cell-line RAW 264.7 (ECACC, 91062702) is cultured in Dulbecco's modified Eagle's medium (DMEM, Sigma–Aldrich, D6546), supplemented with 10% FBS, L-glutamine, and penicillin/streptomycin, and incubated at 37 °C in 5% CO₂ atmosphere.

Keywords:

biosensors · carbon nanotubes · cells · electrochemistry · field-effect transistors

- [1] D. R. Kauffman, A. Star, *Angew. Chem. Int. Ed.* **2008**, *47*, 6550–6570.
- [2] D. R. Kauffman, A. Star, *Chem. Soc. Rev.* **2008**, *37*, 1197–1206.
- [3] B. L. Allen, P. D. Kichambare, A. Star, *Adv. Mater.* **2007**, *19*, 1439–1451.
- [4] C. Dekker, *Phys. Today* **1999**, *52*, 22–28.
- [5] C. Amatore, S. Arbault, M. Guille, F. Lemaître, *Chem. Rev.* **2008**, *108*, 2585–2621.
- [6] S. Rosenblatt, Y. Yaish, J. Park, J. Gore, V. Sazonova, P. L. McEuen, *Nano Lett.* **2002**, *2*, 869–872.
- [7] L. Larrimore, *PhD Thesis* Cornell University 2008.
- [8] I. Heller, A. M. Janssens, J. Männik, E. D. Minot, S. G. Lemay, C. Dekker, *Nano Lett.* **2008**, *8*, 591–595.
- [9] I. Heller, J. Kong, H. A. Heering, K. A. Williams, S. G. Lemay, C. Dekker, *Nano Lett.* **2005**, *5*, 137–142.
- [10] E. D. Minot, A. M. Janssens, I. Heller, H. A. Heering, C. Dekker, S. G. Lemay, *Appl. Phys. Lett.* **2007**, *91*, 093507.
- [11] C. Amatore, S. Arbault, C. Bouton, K. Coffi, J. C. Drapier, H. Ghandour, Y. Tong, *ChemBioChem* **2006**, *7*, 653–661.
- [12] I. Heller, J. Männik, S. G. Lemay, C. Dekker, *Nano Lett.* **2009**, *9*, 377–382.
- [13] S. Arbault, P. Pantano, J. A. Jankowski, M. Vuillaume, C. Amatore, *Anal. Chem.* **1995**, *67*, 3382–3390.
- [14] S. Kasai, H. Shiku, Y. Torisawa, H. Noda, J. Yoshitake, T. Shiraishi, T. Yasukawa, T. Watanabe, T. Matsue, T. Yoshimura, *Anal. Chim. Acta* **2005**, *549*, 14–19.
- [15] B. M. Quinn, S. G. Lemay, *Adv. Mater.* **2006**, *18*, 855–859.
- [16] B. M. Quinn, C. Dekker, S. G. Lemay, *J. Am. Chem. Soc.* **2005**, *127*, 6146–6147.
- [17] T. M. Day, P. R. Unwin, N. R. Wilson, J. V. MacPherson, *J. Am. Chem. Soc.* **2005**, *127*, 10639–10647.
- [18] C. Amatore, S. Arbault, I. Bonifas, R. Lemaître, Y. Verchier, *ChemPhysChem* **2007**, *8*, 578–585.
- [19] C. Amatore, S. Arbault, C. Bouton, J. C. Drapier, H. Ghandour, A. C. W. Koh, *ChemBioChem* **2008**, *9*, 1472–1480.
- [20] I. Heller, J. Kong, K. A. Williams, C. Dekker, S. G. Lemay, *J. Am. Chem. Soc.* **2006**, *128*, 7353–7359.
- [21] R. J. Chen, S. Bangsaruntip, K. A. Drouvalakis, N. W. S. Kam, M. Shim, Y. Li, W. Kim, P. J. Utz, H. Dai, *Proc. Natl. Acad. Sci. USA* **2003**, *100*, 4984–4989.
- [22] K. Besteman, J. O. Lee, F. G. M. Wiertz, H. A. Heering, C. Dekker, *Nano Lett.* **2003**, *3*, 727–730.
- [23] F. J. M. Hoeben, I. Heller, S. P. J. Albracht, C. Dekker, S. G. Lemay, H. A. Heering, *Langmuir* **2008**, *24*, 5925–5931.
- [24] H. A. Heering, K. A. Williams, S. de Vries, C. Dekker, *ChemPhysChem* **2006**, *7*, 1705–1709.
- [25] S. Tsuchiya, Y. Kobayashi, Y. Goto, H. Okumura, S. Nakae, T. Konno, K. Tada, *Cancer Res.* **1982**, *42*, 1530–1536.

Received: May 17, 2009
Revised: July 10, 2009
Published online: